integration with high-speed electronic circuits (*1*, *20*) and the realization of lossless micro-wave links.

References and Notes

1. L. R. Dalton *et al.*, *J. Mater. Chem.* **9**, 1905 (1999); B. H. Robinson *et al.*, *Chem. Phys.* **245**, 35 (1999); W. H. Steier *et al.*, *Chem. Phys.* **245**, 487 (1999); H. S. Nalwa and S. Miyata, Eds., *Nonlinear Optics of Organic Materials and Polymers* (CRC Press, Boca Raton, FL, 1998); J. Zyss, Ed., *Molecular Nonlinear Optics* (Academic Press, New York, 1994); D. L. Wise *et al.*, Eds., *Electrical and Optical Polymer Systems* (Dekker, New York, 1998); P. N. Prasad and D. Williams, *Introduction to Nonlinear Optical Effects in Molecules and Polymers* (Wiley, New York, 1991).
2. W. E. Stephens and T. R. Joseph, *J. Lightwave Technol.* **5**, 380 (1987); C. H. Cox, G. E. Betts, L. M. Johnson, *IEEE Trans. Microwave Theory Tech.* **38**, 501 (1990).
3. C. C. Teng, *Appl Phys. Lett.* **60**, 1538 (1992); D. Chen *et al.*, *Appl Phys. Lett.* **70**, 3335 (1997); H. Fetterman *et al.*, in *Organic Optics and Optoelectronics* (1998 IEEE/LEOS Summer Topical Meeting Digest, Institute of Electrical and Electronic Engineers, New York), pp. 9–10; W. Wang *et al.*, *Appl. Phys. Lett.* **67**, 1806 (1995).
4. K. Naguchi, O. Mitomi, H. Miyazawa, *J. Lightwave Technol.* **16**, 615 (1998).
5. W. K. Burns *et al.*, *IEEE Photon. Technol. Lett.* **10**, 805 (1998).
6. S. R. Marder, D. N. Beratan, L. T. Cheng, *Science* **252**, 103 (1991); S. R. Marder and J. W. Perry, *Science* **263**, 1706 (1994); S. R. Marder *et al.*, *Science* **265**, 632 (1994); D. R. Kanis, M. A. Ratner, T. J. Marks, *Chem. Rev.* **94**, 195 (1994); I. D. L. Albert, T. J. Marks, M. A. Ratner, *J. Am. Chem. Soc.* **119**, 6575 (1997).
7. L. R. Dalton, A. W. Harper, B. H. Robinson, *Proc. Natl. Acad. Sci. U.S.A.* **94**, 4842 (1997).
8. C. Zhang *et al.*, *Polym. Prepr.* **40**, 49 (1999).
9. S. Ermer *et al.*, *Proc. SPIE*, in press.
10. H. Lee *et al.*, *Appl. Phys. Lett.* **71**, 3779 (1997).
11. Y. Shi *et al.*, *IEEE J. Sel. Top. Quantum Electron.* **2**, 289 (1996); Y. Shi, W. Wang, D. J. Olson, W. Lin, J. H. Bechtel, *Proc. SPIE* **3632**, 144 (1999).
12. W. Wang *et al.*, *IEEE Photon. Technol. Lett.* **11**, 51 (1999); T. A. Tumolillo and P. R. Ashley, *IEEE Photon. Technol. Lett.* **4**, 142 (1992); K. H. Hahn *et al.*, *Electron. Lett.* **30**, 1220 (1994).
13. H. R. Janson, *Arch. Elektronik Übertragungstechn.* **32**, 485 (1978).
14. K. D. Singer, M. G. Kuzyk, J. E. Sohn, *J. Opt. Soc. Am. B* **4**, 968 (1987).
15. C. C. Teng, *Appl. Opt.* **32**, 1051 (1993).
16. We have recently realized even lower loss values in partially halogenated materials (for example, 0.7 dB/cm at 1300 nm and 1.0 dB/cm at 1550 nm).
17. Coupling losses of less than 1 dB have been realized by means of exploiting mode size matching techniques and vertical transition waveguide structures [S. M. Garner *et al.*, *IEEE J. Quantum Electron.* **35**, 1146 (1999)]. The total insertion loss of a commercial (Pacific Wave Industries, Los Angeles, CA) EO modulator based on the CLD-1 chromophore is comparable to that of the Lucent lithium niobate modulator.
18. D. Chen *et al.*, *IEEE Photon. Technol. Lett.* **11**, 54 (1999).
19. H. Park, W. Hwang, J. Kim, *Appl. Phys. Lett.* **70**, 2796 (1997); Y. Shi, W. Wang, W. Lin, D. J. Olson, J. H. Bechtel, *Appl. Phys. Lett.* **71**, 2236 (1997).
20. S. Kalluri *et al.*, *IEEE Photon. Technol. Lett.* **8**, 644 (1996).
21. As can be seen from Fig. 2, even modest modification of the structure of CLD-1 can lead to significant improvement in optical nonlinearity. A particularly attractive route to increasing conjugation length while maintaining exceptional thermal and photochemical stability is the insertion of dithiophene units I. Liakatas *et al.*, *Appl. Phys. Lett.*, **76**, 1368 (2000); L. R. Dalton *et al.*, U.S. Patent pending.
22. Research supported by Air Force Research Laboratory, Air Force Office for Scientific Research, Ballistic Missile Defense Organizations, National Science Foundation, and Office of Naval Research.

15 September 1999; accepted 25 February 2000

Dilational Processes Accompanying Earthquakes in the Long Valley Caldera

Douglas S. Dreger,[1]* Hrvoje Tkalčić,[1] Malcolm Johnston[2]

Regional distance seismic moment tensor determinations and broadband waveforms of moment magnitude 4.6 to 4.9 earthquakes from a November 1997 Long Valley Caldera swarm, during an inflation episode, display evidence of anomalous seismic radiation characterized by non–double couple (NDC) moment tensors with significant volumetric components. Observed coseismic dilation suggests that hydrothermal or magmatic processes are directly triggering some of the seismicity in the region. Similarity in the NDC solutions implies a common source process, and the anomalous events may have been triggered by net fault-normal stress reduction due to high-pressure fluid injection or pressurization of fluid-saturated faults due to magmatic heating.

The Long Valley Caldera (LVC) of eastern California (Fig. 1) is tectonically and volcanically active. The 15-km-wide and 30-km-long caldera has produced numerous eruptions since the penultimate event 730,000 years ago that ejected 600 km^3 of rock and formed the caldera through subsequent collapse. The current seismic unrest in the LVC began in 1980 with episodic earthquake swarms and the inflation of a resurgent dome (*1*) (Fig. 1). As a result of this activity the U.S. Geological Survey initiated extensive seismic, ground deformation, and chemical monitoring in 1982. These surveys have revealed episodic seismicity swarms that correlate with the inflation of the resurgent dome, but confirmation of direct fluid involvement in the seismicity has been elusive.

In May 1980, four magnitude (*M*) 6 earthquakes occurred: two south of the LVC in the vicinity of the Hilton Creek fault, and two in the south moat of the caldera (Fig. 1). Two of these events, one located at the caldera margin and the other 12 km to the south, as well as an earlier event in 1978, were found to have significant non–double couple (NDC) seismic moment tensors (*2*).

The latest episode of LVC deformation began in 1997 and first became apparent in two-color laser geodimeter data as increased inflation of the resurgent dome in June followed by earthquake swarm activity in the south moat in July. Deformation rates and swarm activity continued to increase through October to rates exceeding 2 cm/month and 100 $M > 1.2$ earthquakes per day. Swarm activity, strain, and tilt rates increased on 22 November 1997, with the onset of a series of $M > 4$ earthquakes. A

borehole strain meter recorded a transient signal over the next week. Dome inflation, deformation, and swarm activity returned to background rates in early 1998 (*3*).

We investigated anomalous radiation characteristics of the 1997 earthquake swarm using a moment tensor methodology. The seismic moment tensor, Mij, provides a general representation of the seismic source and can be determined by the linear inversion of observed seismic ground motions with appropriately calibrated Green's functions (*4*). Mij is commonly decomposed into double couple (DC), compensated-linear-vector-dipole (CLVD), and isotropic components (*5*), where each of the components of the moment tensor decomposition is represented as a percentage of the total (*6*). The DC consists of two vector dipoles of equal magnitude but opposite sign, resolving shear motion on faults oriented 45° to the principle eigenvectors of Mij. The CLVD consists of a major vector dipole with twice the strength and opposite sign to two orthogonal, minor vector dipoles and can describe the separation or compression of a fault with no net volume change. The isotropic component has three orthogonal vector dipoles of equal magnitude and resolves volumetric changes.

NDC seismic moment tensors have been observed in a variety of tectonic and volcanic environments. Several mechanisms such as multiplanar rupture (*7*, *8*), nonplanar rupture (*9*), and tensile failure (*10*) have been proposed to explain observed NDC moment tensors. In principle it should be possible to determine the isotropic components given body and surface wave data; however, they are difficult to resolve (*11*), and only a few studies have reported significant volumetric components (*12*, *13*).

Routine analysis of seismic moment tensors by the Berkeley Seismological Laboratory revealed that a number of events in the November 1997 swarm displayed unusual seismic radiation patterns (*14*). Seven events (Table 1) have

[1]Berkeley Seismological Laboratory, University of California, Berkeley, CA 94720, USA. [2]U.S. Geological Survey, Menlo Park, CA 94025, USA.

*To whom correspondence should be addressed at Berkeley Seismological Laboratory, 281 McCone Hall, University of California, Berkeley, CA 94720, USA. E-mail: dreger@seismo.berkeley.edu

been reanalyzed with our method, which inverts three-component, complete seismograms (including regional *P* and *S* body waves and Love and Rayleigh surface waves), recorded at the five closest Berkeley Digital Seismic Network stations (Fig. 1), for the complete seismic moment tensor (*4*). As an example of the inverse procedure we compare the deviatoric and full moment tensor (FMT, including isotropic com-

ponents) solutions for EVT4 (Fig. 2, A and B). We typically find that CLVD components are ≤30% for earthquakes in Northern California. The deviatoric inversion (Fig. 2A) yielded an anomalous solution with a 67% CLVD component, while the FMT solution (Fig. 2B) shows a large 42% isotropic moment, the sign of which indicates volumetric expansion. In contrast, the deviatoric inversion for EVT6 yielded a nearly

pure DC solution and the FMT inversion yielded a large DC component (Table 2 and Fig. 2, C and D). Four events, EVT1−4, were found to have anomalous NDC moment tensors including large dilatational volumetric components, and three, EVT5−6 and REF1, resulted in nearly pure DC solutions (Table 2). Tests of inversion sensitivity, forward modeling of the data, examination of Poisson ratio sensitivity, and three-CLVD decompositions of deviatoric inversion results indicate that there is no trade-off between a vertical-CLVD and the isotropic component that we report.

To estimate the significance of the deviatoric and FMT solutions, we evaluated the improvement in fit to the data using the *F* test (*15*) (Table 2). A grid search algorithm was used to determine the best pure DC solution for each event. The FMT solutions of the anomalous events (EVT1−4) satisfy the *F* test for significance above the 95% level relative to a reference DC solution. The *F* test using the deviatoric solution as reference indicates >90% significance for EVT1 and >95% significance for EVT2−4. The FMT solution for these four events resulted in isotropic moments that are a considerable fraction of the deviatoric moment, and the improvement in fit is statistically significant whether the DC or the deviatoric NDC
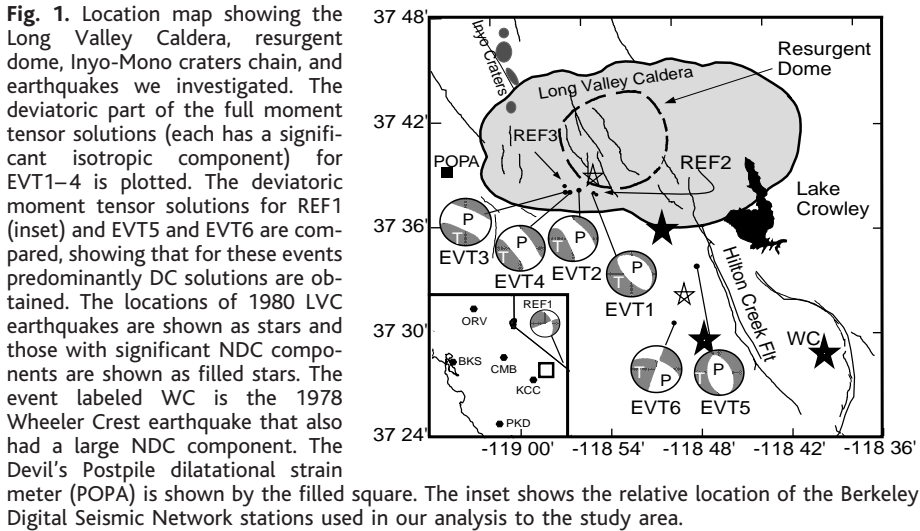
Fig. 1. Location map showing the Long Valley Caldera, resurgent dome, Inyo-Mono craters chain, and earthquakes we investigated. The deviatoric part of the full moment tensor solutions (each has a significant isotropic component) for EVT1−4 is plotted. The deviatoric moment tensor solutions for REF1 (inset) and EVT5 and EVT6 are compared, showing that for these events predominantly DC solutions are obtained. The locations of 1980 LVC earthquakes are shown as stars and those with significant NDC components are shown as filled stars. The event labeled WC is the 1978 Wheeler Crest earthquake that also had a large NDC component. The Devil's Postpile dilatational strain meter (POPA) is shown by the filled square. The inset shows the relative location of the Berkeley Digital Seismic Network stations used in our analysis to the study area.
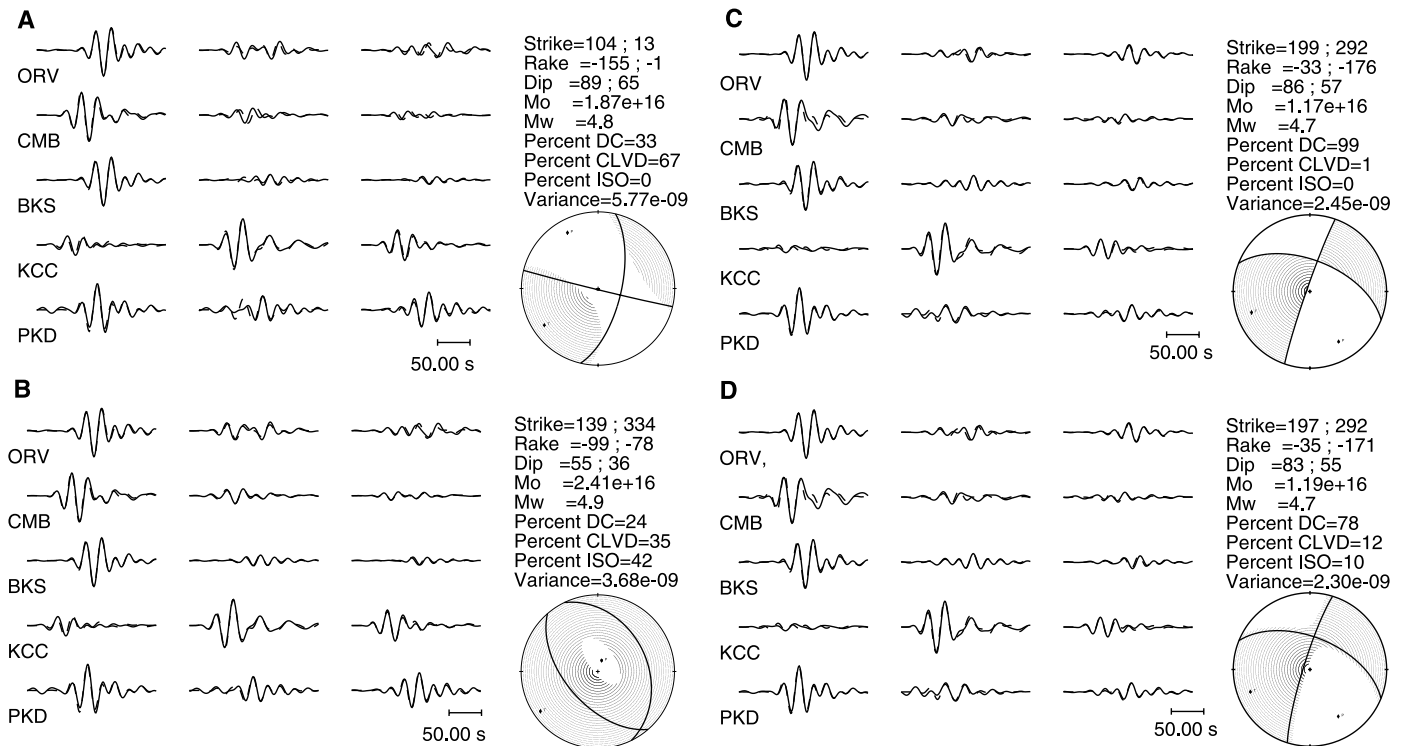

Fig. 2. Comparison of the deviatoric (**A**) and full moment tensor (**B**) inversion results for EVT4. In both cases, three-component (transverse, radial, and vertical, from left to right) displacement data (solid line) are compared to synthetic seismograms (dashed line). The station azimuth and maximum trace amplitudes are (314°, 5.16×10^{-4} cm), (290°, 1.23×10^{-3} cm), (276°, 1.03×10^{-3} cm), (223°, 2.05×10^{-3} cm), and (218°, 6.99×10^{-4} cm) for ORV, CMB, BKS, KCC, and PKD, respectively. The strike, rake, and dip of the two nodal planes of the best double couple, the scalar seismic moment (Mo), moment magnitude (Mw), the percent double couple (DC), percent compensated linear vector dipole (CLVD), percent isotropic (ISO), the variance of the data to the model, and lower hemisphere projection of the *P*-wave radiation pattern are provided. The same data are compared for EVT6 in (**C**) and (**D**). The station azimuth and maximum trace amplitude for EVT6 are (315°, 3.03×10^{-4} cm), (294°, 9.41×10^{-4} cm), (279°, 3.93×10^{-4} cm), (245°, 9.49×10^{-4} cm), and (222°, 3.90×10^{-4} cm) for ORV, CMB, BKS, KCC, and PKD, respectively.

Table 1. Earthquake data reported in the Council of the National Seismic System (CNSS) catalog

Event ID	Date (day/month/year)	Origin time (UTC)	Latitude (deg. N)	Longitude (deg. W)	Depth* (km)	Depth† (km)	Magnitude
REF1	02/11/1997	08:51:53.9	37.846	−118.215	6.4	8	5.3
EVT1	22/11/1997	12:06:56.0	37.635	−118.917	8.4	8	4.6
REF2	22/11/1997	16:09:08.7	37.632	−118.916	8.0	–	2.9‡
EVT2	22/11/1997	17:20:35.1	37.636	−118.936	7.7	5	4.9
EVT3	22/11/1997	18:10:59.4	37.634	−118.951	8.2	8	4.6
REF3	23/11/1997	02:19:50.4	37.640	−118.952	7.4	–	3.7‡
EVT4	30/11/1997	21:17:05.4	37.634	−118.946	7.1	5	4.9
EVT5	15/07/1998	04:53:19.3	37.564	−118.806	6.2	5	5.0
EVT6	15/05/1999	17:54:08.8	37.509	−118.831	7.3	8	4.7

*Hypocental depths reported in the CNSS catalog.　　†Depths obtained by moment tensor inversion.　　‡Local magnitude; all others are moment magnitude.

Table 2. Comparison of the deviatoric and full moment tensor inversion results. The percentages of DC, CLVD, and ISO (6) to the left are for the deviatoric inversions and to the right for the full moment tensor inversions. The deviatoric M_0 for the full moment tensor inversion is given. $F_{NDC} = \sigma^2_{DC}/\sigma^2_{NDC}$, $F_{Full} = \sigma^2_{DC}/\sigma^2_{Full}$, $F = \sigma^2_{NDC}/\sigma^2_{Full}$ are the F statistics comparing the DC to deviatoric, the DC to full, and deviatoric to full moment tensor solutions, respectively (15). Maximum critical values of F to exceed are 1.24, 1.36, and 1.55 for confidence levels of 90, 95, and 99%, respectively.
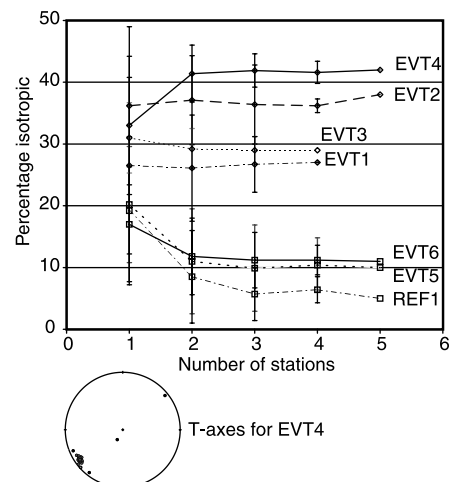
| Event ID	DC (%)	CLVD (%)	ISO (%)	Deviatoric M_0 (10^{16} N m)	F_{NDC}	F_{Full}	F	ΔV (km³)	L (km)	U_N (cm)
REF1	100/93	0/2	0/5	9.88	–	1.00	–	–	–	–
EVT1	77/71	23/3	0/27	0.90	1.42	1.96	1.31	7.2×10^{-5}	1.48	3.3
EVT2	59/34	41/32	0/33	2.49	1.22	2.06	1.70	2.4×10^{-4}	1.59	9.5
EVT3	13/27	87/44	0/29	0.78	2.35	3.59	1.53	6.4×10^{-5}	1.02	6.1
EVT4	33/24	67/35	0/42	2.41	1.48	2.33	1.57	3.4×10^{-4}	1.79	10.6
EVT5	98/80	2/9	0/11	3.11	–	1.01		–	–	–
EVT6	99/78	1/12	0/10	1.19	–	1.07		–	–	–

Fig. 3. Jackknife test illustrating the stability of the isotropic component for the three anomalous events (diamonds) compared to that for the DC events (squares) as a function of the number of stations used in the inversion. The symbols show the mean percent ISO ± 1 SD (error bars). The sign of the volumetric component is dilation for EVT1–4 and EVT5–6, and compression for REF1. The orientation of the T axes for all of the station permutations for EVT4 is quite stable (inset); however, several of the single-station inversions deviate from the main cluster of T axes.

solution is used as a reference (Table 2). The maximum eigenvalue for all of the inversions is extensional, and the corresponding eigenvectors are nearly horizontal and oriented to the southwest. This orientation is consistent with regional strain and the inflation of the resurgent dome that is observed in the LVC (1). Deviatoric inversions for EVT5 and EVT6 resulted in large DC components, and the FMT inversions resulted in isotropic components of 12% or less and large DC components. The F tests for EVT5–6 indicate that the reduction in variance is not statistically significant above 95%, and in fact, it is only significant at the 65% level at best. REF1 located outside of the LVC is another event with a small, statistically insignificant, isotropic component.

For additional insight into the significance of the results, we tested the stability of the solutions using subsets of the data to explore the possibility that a given station or combination of stations may be controlling the inversion. In our Jackknife test, we performed inversions using all combinations of one, two, three, four, and five stations for the LVC events (Fig. 3) and found a clear separation between the anomalous events that satisfied the F test and the reference events that did not. The reference events with small isotropic components (~10%) indicate that it is not possible to resolve isotropic components of 10% or less. The mean value of the isotropic percentage for

EVT1–4 lies between 27 and 45% and is stable for all of the station subsets. The stability of one- and two-station inversions indicates that azimuthally dependent path effects are not a factor in the inversion results of the anomalous events. The stability of the four-station inversions reveals that the isotropic component is not due to the dominance of any one station.

Broadband P waveforms also show anomalous behavior (Fig. 4). REF2 and REF3 are small events that have similar P waveforms and first-motion focal mechanisms, indicating that the observed P-wave complexity may be due to path effects. Although it is possible that the complex P waveform of these events is due to an identical source process, this is unlikely, and the first P pulse is interpreted as direct P, and the two that follow are likely reflected arrivals or mode conversions. Assuming a constant stress-drop scaling law and a value of 3 MPa, a source duration of 0.2 s is obtained for REF3 and 0.06 s for REF2 (16). The observed duration of the direct P pulse is the same for the two events, suggesting that seismic-wave attenuation may be broadening the pulses. EVT6 resulted in a nearly pure DC solution that is similar to the first-motion solutions of REF2 and REF3 and is also seen to have a similar P waveform. The estimated source duration of 0.46 s, for a stress drop of 3 MPa, is consistent with the observed duration of 0.5 s, indicating that for the larger events, the duration of the P waves is a good

representation of the source process time.

The P waveforms of EVT1, EVT2, and EVT4 have unusually long duration. There is a 2- to 2.5-s source phase with superimposed shorter period arrivals. Estimated static stress drops based on these long source durations are ≪0.1 MPa and are outside the 1- to 10-MPa range observed in most earthquakes (17). For example, assuming a stress drop of 3 MPa, a duration of 0.58 s is obtained, which is less than a third of the observed duration. EVT3 is an anomalous moment tensor event that has an emergent onset to the P waveform, but does not have the long-period source component observed in the other three events.

The isotropic moment was used to estimate the change in source volume (ΔV) through the equation, $M_{0iso} = [\lambda + (2/3)\mu]\Delta V$ (18), where M_{0iso} is the scalar seismic moment of the isotropic component, and λ and μ are the Lame and rigidity elasticity constants. Assuming that $\lambda = \mu = 3 \times 10^{10}$ Pascal, the estimated values of ΔV (Table 2) are much less than the 0.02 to 0.04 km³/year that can be attributed to the inflation of the resurgent dome (14). For a spherical geometry, the radii of the volume increase are 28, 39, 25, and 43 m for EVT1–4. Assuming a static stress drop of 3 Mpa, the fault dimension, L, of each event was determined from the deviatoric seismic moment (16), and the fault separation, $U_N = \Delta V/L^2$, was estimated (Table 2). U_N is on the order of 5 to 10 cm, which is consistent with observed openings of exhumed magmatic dikes; however, U_N
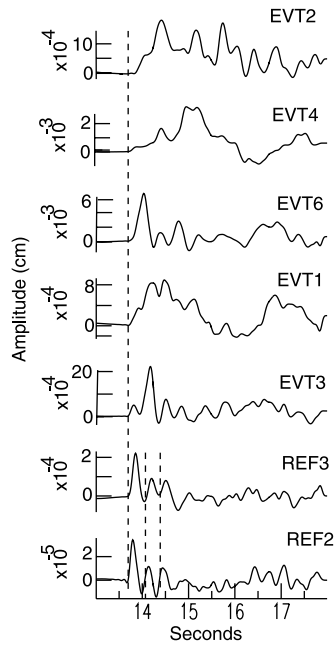
Fig. 4. Vertical component *P* waveforms recorded at the closest station, KCC. The displacement data have been bandpass-filtered between 0.10 and 8.0 Hz and are organized in order of increasing seismic moment from bottom to top. The long dashed lines mark the direct arrival, and the short dashed lines show arrivals that are interpreted to result from Earth structure effects.

is inversely proportional to L^2 and is therefore subject to uncertainty. For example, a stress drop of 0.1 MPa results in separations of between 0.5 to 1 cm.

An anomalous compressional volume strain transient was observed during this sequence on the POPA dilatational strain meter located 11 to 13 km to the west of the study events (Fig. 1). This exponential-like strain event (Fig. 5) apparently initiated with EVT1 at 12:06 UTC on 22 November and decayed with a 2.3-day time constant. Coseismic extensional strain steps of −3.5, −6.3, and −19 nanostrain were observed with events EVT1, EVT2, and EVT3, respectively. EVT4 on 30 November produced a coseismic compressional strain step of 37 nanostrain with no additional transient nature. Coseismic strain offsets usually agree with calculations based on moment release by earthquakes (*19*). Coseismic offsets for all events are about a factor of 2 or greater than offsets calculated for POPA, assuming simple DC dislocations. These independent data support the contention that significant volume change occurred with these later earthquakes. Inclusion of the volume components inferred above into the offset calculation reduces the discrepancy but still underestimates the observed offsets. This suggests that additional volumetric moment release occurred outside the pass band of the seismometers.

It has been suggested that NDC moment
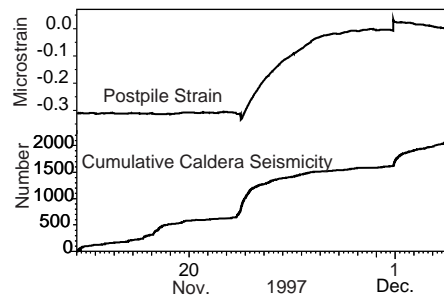
Fig. 5. Comparison of dilatational strain observed at Devil's Postpile (POPA, Fig. 1) with cumulative *M* > 1.5 seismicity in the south moat of LVC. Three steps in cumulative seismicity are observed. The step in seismicity on 22 November is seen to correlate well with a compressional strain transient.

tensors for the 1980 events could be due to tensile failure resulting from injection of high-pressure fluid (*10*), simultaneous fault slip of two differently oriented DC sources (*7*), and bias due to unaccounted for near-source crustal structure (*7*). None of these studies allowed for an isotropic component, and it is not known if the 1980 and 1997 events are similar in this regard; however, they are quite similar in terms of the NDC deviatoric moment tensor solutions.

The observation of significant volumetric expansion components in the moment tensors of 1997 LVC seismicity indicates a direct relation between at least some of the seismicity and hydrothermal or magmatic processes. Magma intrusion rapid enough to cause the May 1980 events cannot be ruled out (*10*); however, the source process times of the 1997 events, although unusually long, are too short to be explained by the injection of low-viscosity magma. The isotropic components may be due to the injection of high-pressure fluids or pressurization of a fluid-saturated fault by heat from a nearby magmatic body. A northeast-dipping dike from just north of the south moat of the caldera is one possible model that can explain the transient dilatational strain anomaly of 22 November 1997 (*3*). The modeled dike fails to bisect the faults in the south moat, and a direct interaction seems unlikely, although it is possible that a network of fractures may allow effective fluid and heat transport. Right-lateral shear on an east-west striking fault coupled with a minor inflation source can also explain the strain data (*3*), and a possible scenario for the recent LVC activity is the evolution of the system from a locked fault, to stick-slip motion, to stable-sliding as fault pore pressure increases.

References and Notes

1. D. P. Hill, R. A. Bailey, A. S. Ryall, *J. Geophys. Res.* **90**, 11111 (1985).
2. J. W. Given, T. C. Wallace, H. Kanamori, *Bull. Seismol. Soc. Am.* **72**, 1093 (1982); G. Ekstrom, *Eos* **64**, 769 (1983); G. Ekstrom and A. M. Dziewonski, *Eos* **64**, 262 (1983); B. R. Julian, *Nature* **303**, 323 (1983); J. S. Barker and C. A. Langston, *Bull. Seismol. Soc. Am.* **73**, 419 (1983); T. Wallace, J. Given, H. Kanamori, *Geophys. Res. Lett.* **9**, 1131 (1982).
3. J. Langbein, S. Wilkinson, J. Feinberg, M. Johnston, *Eos* **79**, E963 (1998); D. P. Hill, *Eos* **79**, E949 (1998).
4. The method used inverts complete, three-component, long-period (50 to 20 s) displacement seismograms for the six independent elements of the symmetric seismic moment tensor. A synchronous and impulsive source time function, and spatial point-source are assumed. A linear inversion for moment tensor amplitudes is then possible. The event source depth is determined iteratively by performing independent inversions for depths of 5, 8, 11, 14, and 17 km. See, for example, D. S. Dreger and D. V. Helmberger, *J. Geophys. Res.* **98**, 8107 (1993); M. E. Pasyanos, D. S. Dreger, B. Romanowicz, *Bull. Seismol. Soc. Am.* **86**, 1255 (1996).
5. L. Knopoff and M. J. Randall, *J. Geophys. Res.* **75**, 4957 (1970); M. L. Jost and R. B. Hermann, *Seismol. Res. Lett.* **60**, 37 (1989).
6. The percent CLVD is calculated from the minimum and maximum eigenvalues defined by ($|\lambda_3| > |\lambda_2| > |\lambda_1|$), where $\varepsilon = |\lambda_1/\lambda_3|$, and $PCLVD = 200\varepsilon$ and $PDC = 100 - 200\varepsilon$. The percent isotropic (ISO) is the ratio of the isotropic moment to the sum of the isotropic and deviatoric moments.
7. T. C. Wallace, *J. Geophys. Res.* **90**, 11171 (1985).
8. K. Kuge and T. Lay, *J. Geophys. Res.* **99**, 15457 (1994).
9. C. Frohlich, *Science* **264**, 804 (1994).
10. B. R. Julian and S. A. Sipkin, *J. Geophys. Res.* **90**, 11155 (1985).
11. H. Kawakatsu, *Geophys. J. Int.* **126**, 525 (1996); H. Dufumier and L. Rivera, *Geophys. J. Int.* **131**, 595 (1997).
12. T. Zheng, Z. Yao, P. Liu, *Phys. Earth Planet. Int.* **91**, 285 (1995); P. Campus, P. Suhadolc, G. F. Panza, J. Sileny, *Tectonophysics* **261**, 147 (1996); T. Hara, K. Kuge, H. Kawakatsu, *Geophys. J. Int.* **127**, 515 (1996).
13. A. D. Miller, G. R. Foulger, B. R. Julian, *Rev. Geophys.* **36**, 551 (1998).
14. U. S. Geological Survey Volcano Hazards Program, Long Valley Caldera Monitoring Report, 1997.
15. It is possible to fit the data better with models that have a greater number of unknowns. The *F* test is used to determine whether a model with a change in the number of free parameters fits the data significantly better than might be expected from random fluctuations in the data [W. Menke, *Geophysical Data Analysis: Discrete Inverse Theory* (Academic Press, New York, 1989), pp. 96–97. There are five unknowns in the DC inversions (depth, scalar seismic moment, strike, rake, and dip), six in the deviatoric moment tensor inversion, and seven in the full moment tensor inversion. To perform the test, the variance, σ^2, of the data is estimated from the model prediction error, $e_i = (data_i - synthetic_i)$, where $\sigma^2 = \Sigma e_i^2/(N - M)$ and *N* and *M* are the number of observations and model parameters, respectively. The *F* statistic is the ratio of the two data variance estimates. Critical values of *F* above which the difference in the variance is significant can be calculated from the *F* distribution. For the calculations in this report, considering a 20-s correlation length for the data, the critical values of *F* are 1.36 (95% confidence) and 1.55 (99% confidence).
16. Given the definitions of scalar seismic moment, $M_0 = \mu AD$, and static stress drop, $\Delta\sigma = c\mu D/L$, where μ is the material rigidity at the source, *A* (equal to L^2) is the source area, and *D* is the average slip, *L* is the source dimension, and *c* is a geometrical constant approximately equal to 1, the following relationship for *L* is found: $L \approx (M_0/\Delta\sigma)^{1/3}$. The source duration τ is then found to approximately equal $(M_0/\Delta\sigma)^{1/3}/\beta$, where β is the seismic shear-wave velocity.
17. H. Kanamori and D. Anderson, *Bull. Seismol. Soc. Am.*, **65**, 1073 (1975).
18. K. Aki and P. Richards, *Quantitative Seismology, Theory and Methods* (Freeman, San Francisco, 1980), p. 932.
19. M. J. S. Johnston, A. T. Linde, M. T. Gladwin, R. D. Borcherdt, *Tectonophysics* **144**, 189 (1987).
20. This is contribution 00-02 of the Berkeley Seismological Laboratory.

4 November 1999; accepted 23 February 2000